

cy.1

**AERODYNAMIC CHARACTERISTICS OF
DISK-GAP-BAND PARACHUTES IN THE
WAKE OF VIKING ENTRY FOREBODIES
AT MACH NUMBERS FROM 0.2 TO 2.6**



David E. A. Reichenau

ARO, Inc.

Property of U. S. Air Force
July 1972
AEDC LIBRARY
F40600-73-C-0004

Approved for public release; distribution unlimited.

**PROPULSION WIND TUNNEL FACILITY
ARNOLD ENGINEERING DEVELOPMENT CENTER
AIR FORCE SYSTEMS COMMAND
ARNOLD AIR FORCE STATION, TENNESSEE**

AEDC TECHNICAL LIBRARY



5 0720 00033 3700

NOTICES

When U. S. Government drawings specifications, or other data are used for any purpose other than a definitely related Government procurement operation, the Government thereby incurs no responsibility nor any obligation whatsoever, and the fact that the Government may have formulated, furnished, or in any way supplied the said drawings, specifications, or other data, is not to be regarded by implication or otherwise, or in any manner licensing the holder or any other person or corporation, or conveying any rights or permission to manufacture, use, or sell any patented invention that may in any way be related thereto.

Qualified users may obtain copies of this report from the Defense Documentation Center.

References to named commercial products in this report are not to be considered in any sense as an endorsement of the product by the United States Air Force or the Government.

**AERODYNAMIC CHARACTERISTICS OF
DISK-GAP-BAND PARACHUTES IN THE
WAKE OF VIKING ENTRY FOREBODIES
AT MACH NUMBERS FROM 0.2 TO 2.6**

**David E. A. Reichenau
ARO, Inc.**

Approved for public release; distribution unlimited.

FOREWORD

The work reported herein was done at the request of the National Aeronautics and Space Administration (NASA), Langley Research Center, Hampton, Virginia, under Program Element 921E.

The test results presented were obtained by ARO, Inc. (a subsidiary of Sverdrup & Parcel and Associates, Inc.), contract operator of the Arnold Engineering Development Center (AEDC), Air Force Systems Command (AFSC), Arnold Air Force Station, Tennessee, under Contract F40600-73-C-0004. The test was conducted in Tunnel 16T from June 29 to July 3, 1971, and in Tunnel 16S from August 12 to 13, 1971, under ARO Project No. PT1057. The manuscript was submitted for publication on October 8, 1971.

This technical report has been reviewed and is approved.

R. W. WORKING

Major, USAF

Chief Air Force Test Director, PWT

Directorate of Test

A. L. COAPMAN

Colonel, USAF

Director of Test

ABSTRACT

Tests were conducted in the Propulsion Wind Tunnels (16T) and (16S) to determine the drag and performance characteristics of various disk-gap-band parachute configurations in the wake of a 0.10-scale Viking entry vehicle. The parachutes were also tested behind a small faired body to obtain minimum interference parachute performance characteristics. The results show that in general the parachutes had good inflation and stability characteristics in the wake of the entry forebodies at Mach numbers from 0.2 to 0.8 and from 1.2 to 2.0. Considerable loss in parachute performance was experienced in the wake of the forebodies in the vicinity of Mach number 1.0. Increasing the parachute trailing distance and suspension line length increased the parachute drag coefficient at each Mach number.

CONTENTS

	<u>Page</u>
ABSTRACT	iii
NOMENCLATURE	v
I. INTRODUCTION	1
II. APPARATUS	
2.1 Test Facility	1
2.2 Test Article	1
2.3 Instrumentation	2
III. PROCEDURE	2
IV. RESULTS AND DISCUSSION	
4.1 Parachute Dynamic Characteristics	3
4.2 Parachute Steady-State Performance	4
V. CONCLUDING REMARKS	4

APPENDIXES

I. ILLUSTRATIONS

Figure

1. Sketch of Model Installation	9
2. Installation Photographs	10
3. Major Model Details	14
4. Photograph of Parachute Attachment	17
5. Disk-Gap-Band Parachute Assembly	18
6. Photographs of the Disk-Gap-Band Parachute at Various Trailing Distances and Mach Numbers	21
7. Effect of Forebody Shape on the Parachute Drag Coefficient, $S/D_o = 1.85$, $X/d = 9.14$	23
8. Variation of Parachute Drag Coefficient with Free-Stream Mach Number	24

II. TABLE

I. Summary of Parachute Test Conditions and Performance Results	27
--	----

NOMENCLATURE

A	Model reference area, sq ft
C_{D_o}	Parachute drag coefficient, $F_P/q_\infty S_o$
D_o	Parachute nominal diameter, 5.3 ft

d	Model reference diameter, 1.15 ft
F_p	Parachute drag force, lb
M_∞	Free-stream Mach number
q_∞	Free-stream dynamic pressure, psf
R	Riser line length, ft
S	Suspension line length, ft
S_o	Parachute reference area (based on nominal diameter), 22.06 sq ft
S/D_o	Ratio of parachute suspension line length to parachute nominal diameter
X	Axial distance between the entry vehicle and the parachute inlet, ft
X/d	Parachute trailing distance

SECTION I INTRODUCTION

The purpose of the series of tests conducted in the Propulsion Wind Tunnels (16T) and (16S) was to determine the drag and performance characteristics of various disk-gap-band (DGB) parachute configurations in the wake of 0.10-scale Viking entry forebodies. The DGB parachutes were also tested behind a strut-mounted small faired body to provide minimum interference performance characteristics. The tests consisted of variations of both the parachute assembly trailing distance and suspension line length. Data were obtained at Mach numbers from 0.2 to 2.6 at a free-stream dynamic pressure of 80 psf.

SECTION II APPARATUS

2.1 TEST FACILITY

Tunnels 16T (transonic) and 16S (supersonic) are continuous flow, closed-circuit wind tunnels capable of being operated within a Mach number range from 0.2 to 1.5 and 1.5 to 4.75, respectively. Tunnel 16T can be operated within a stagnation pressure range from 120 to 4000 psfa depending on the Mach number, and Tunnel 16S can be operated within a stagnation pressure range from 200 to 2000 psfa depending on the Mach number. The stagnation temperature can be varied from approximately 80 to a maximum of 160°F in Tunnel 16T and from approximately 100 to a maximum of 620°F in Tunnel 16S. The specific humidity of the air in both wind tunnels is controlled by removing tunnel air and supplying conditioned makeup air from an atmospheric dryer. A more complete description of the wind tunnels and their operating characteristics is contained in the Test Facilities Handbook.¹

2.2 TEST ARTICLE

A sketch showing the model location in the wind tunnel test section is shown in Fig. 1 (Appendix I), and installation photographs of the models and the strut support system are presented in Fig. 2. The model represents a 0.10-scale entry vehicle with a maximum diameter of 13.8 in. The model had provisions to remove the 140-deg conical aeroshell and to install a representation of the Viking Lander Capsule (Fig. 2c). Major model details and dimensions of these models and the faired body are presented in Fig. 3.

The model was attached to the strut support arrangement through two internally mounted load cells that provided the entry vehicle drag and the combined entry vehicle-parachute drag, respectively. The parachutes were packed in a deployment bag and stowed in a tube mounted near the lower portion of the support strut. The suspension lines were led up the strut trailing edge and tied with break cord which severed as the

¹Test Facilities Handbook (Ninth Edition). "Propulsion Wind Tunnel Facility, Vol. 4." Arnold Engineering Development Center, July 1971.

parachute was pneumatically deployed from the stowage tube. The parachute suspension lines were attached to the model through a swivel-tensiometer-bridle arrangement. A photograph showing the aft portion of the model and the bridle attachment is presented in Fig. 4.

Major dimensions and geometric properties of the DGB parachutes are shown in Fig. 5. The parachutes were constructed of Dacron[®] cloth (2.1 oz/yd²), and the suspension lines were made of 200-lb-test braided nylon. All the DGB parachutes had a porosity of 12.5 percent and a nominal diameter of 5.3 ft. The parachute trailing distances were increased by increasing the suspension line lengths except for Configuration 2 behind the entry vehicle which increased the trailing distance by adding a 45.8-in. riser line.

2.3 INSTRUMENTATION

Load cells of 500- and 2000-lb capacity were used to measure the entry vehicle drag and the entry vehicle plus parachute drag, respectively, with an accuracy of ± 30 lb. Also, a 2000-lb capacity tensiometer was used to measure the parachute drag. Motion-picture and television cameras, installed in the test section walls, were used to document and monitor the test.

The outputs from the two load cells and the tensiometer were digitized and permanently recorded on magnetic tape for on-line data reduction. These outputs were also continuously recorded on direct-writing and film pack oscillographs for monitoring the model and parachute dynamics.

SECTION III PROCEDURE

The parachute package, which consists of a parachute enclosed in a deployment bag, was packed in a tube mounted on the model support strut before wind tunnel test operation was initiated. Once the desired test conditions were established, a countdown sequence procedure was used for data acquisition during parachute deployment. The deployment procedure consisted of activating the recording oscillographs, the test section cameras, and the analog tape recording system followed by pneumatically ejecting the parachute-bag combination into the airstream. Upon completion of the parachute deployment sequence, steady-state drag loads were calculated by averaging the analog output from the load cells and tensiometer over 1-sec intervals.

DGB parachutes of various S/D_0 (ratio of suspension line length to parachute nominal diameter) values were tested at various X/d locations through the Mach number range from 0.2 to 2.6 at nominal free-stream dynamic pressures of approximately 80 psf. The parachutes were deployed at various Mach numbers, and after data acquisition was completed, the parachute performance was investigated at other Mach numbers. In some instances when the parachute failed, a backup parachute was deployed and additional data were obtained until the desired Mach number range was covered for that parachute configuration. A summary of the test conditions established for each parachute configuration is presented in Table I (Appendix II).

SECTION IV

RESULTS AND DISCUSSION

The primary purpose of this investigation was to determine the drag performance of the disk-gap-band (DGB) parachutes operating in the wake of the Viking Entry Vehicle (EV) or Lander (L) forebodies at various trail distances. The parachute performance was also obtained behind a small faired body to determine the parachute performance with minimum wake interference.

The data obtained from the tensiometer, which measures parachute drag only, are presented for the Mach number range from 0.2 to 1.4. The tensiometer malfunctioned during the Tunnel 16S test. Parachute drag was determined from the difference between the two load cells which measured the model axial loads and the model-plus-parachute axial loads at Mach numbers from 1.8 to 2.6. Tensiometer data before failure are presented at Mach number 2.2 for comparison.

4.1 PARACHUTE DYNAMIC CHARACTERISTICS

The parachute stability and inflation characteristics were visually evaluated from the motion pictures. Observations of the parachute performance for each test condition are presented in Table I. In general, the parachute configurations trailing the forebodies were well inflated and stable (oscillations less than 6 deg) or very stable (oscillations less than 3 deg) for the Mach number range from 0.2 to 0.8 and from 1.2 to 2.0. Unstable conditions were noted in the Mach number range from 0.9 to 1.1 and from 2.1 to 2.6, especially for the parachute configurations with the smaller X/d values. At the unstable conditions, the parachute exhibited underinflation with excessive canopy and suspension line dynamics resulting in a loss in drag.

Increasing the value of X/d reduced the parachute dynamics, and each parachute configuration had essentially the same performance trends when operating at the same trailing distance behind the forebodies. Sporadic pulsing of the parachute canopy occurred throughout the range of test conditions for the parachute configurations with X/d less than nine in the wake of the Viking forebodies. This effect was generally greater for the high Mach numbers and smaller trailing distances.

Canopy inflation and stability characteristics of the parachute were very good at all test conditions and trailing distances behind the faired body. Configuration 5 with an S/D_0 of 1.85 exhibited the best inflation and stability characteristics of the four configurations tested behind the faired body. At Mach numbers of 1.2, 1.3, and 1.4, Configuration 5 exhibited the performance characteristics of an ideal parachute with no oscillations or distorting moments to disturb the parachute from its equilibrium position. None of the four parachute configurations trailing the faired body exhibited the unstable conditions in the vicinity of $M_\infty = 1.0$ as was noted for the parachute configurations trailing the forebodies. Photographs of various parachute configurations in the wake of the three forebodies are shown in Fig. 6 for a range of Mach numbers from 0.6 to 1.4.

4.2 PARACHUTE STEADY-STATE PERFORMANCE

The effects of the forebody shape on the parachute drag coefficient at $X/d = 9.14$ are presented in Fig. 7. At a given Mach number, the forebody wake effect produced by the entry vehicle and the lander resulted in essentially the same parachute drag coefficients. The parachute drag coefficient obtained in the wake of the forebodies in the vicinity of $M_\infty = 1.0$ was substantially less than the drag coefficient obtained behind the faired body. At $M_\infty = 1.0$, the parachute underinflation caused by the forebody wake resulted in parachute drag reductions of approximately 30 percent when compared to the drag coefficient obtained behind the faired body with minimum wake interference.

The variation of parachute drag coefficient with Mach number at various values of X/d are presented in Fig. 8. For a given Mach number, the parachute drag coefficient increased with increasing X/d locations behind the Viking forebodies as shown in Figs. 8a and b, respectively. These data also show a considerable decrease in drag coefficient with Mach number as the Mach number approached 1.0, especially for the parachute configurations with the smaller X/d locations. Increasing the Mach number from 0.6 to 1.0 resulted in as much as 50-percent reduction in parachute drag coefficient as the parachute became underinflated in the wake of the forebody. Two parachute configurations (Configurations 2 and 4) were tested in the Mach number range above 1.8 in the wake of the entry vehicle. The drag coefficient for Configuration 4 with $X/d = 8.53$ decreased approximately 28 percent as the Mach number was increased from 1.8 to 2.6. The drag coefficient for Configuration 2 with $X/d = 6.50$ remained essentially the same in the Mach number range from 1.8 to 2.2. The parachutes were tested behind a faired body to obtain relatively interference-free parachute drag characteristics. As shown in Fig. 8c, increasing the value of S/D_0 also increased the parachute drag coefficient at a given Mach number behind the faired body.

SECTION V CONCLUDING REMARKS

Tests were conducted to determine the drag and performance characteristics of disk-gap-band parachute configurations with various trailing distance and suspension line lengths. The parachutes, attached to 0.10-scale Viking entry forebodies and a faired body, were investigated in the Mach number range from 0.2 to 2.6 at a nominal free-stream dynamic pressure of 80 psf. The following observations are a result of these tests:

1. Canopy inflation and stability were very good at all test conditions behind the faired body.
2. In general, the parachute had good inflation and stability characteristics in the wake of the entry vehicle and lander forebodies at Mach numbers from 0.2 to 0.8 and from 1.2 to 2.0.
3. Considerable loss in performance of the parachute was experienced in the wake of the Viking forebodies in the vicinity of Mach number 1.0.

4. Increasing the parachute trailing distance increased the parachute drag coefficient at each Mach number.
5. Increasing the Mach number from 0.6 to 1.0 resulted in as much as 50-percent reduction in parachute drag coefficient as the parachute became underinflated in the wake of the Viking forebodies.

APPENDIXES
I. ILLUSTRATIONS
II. TABLE

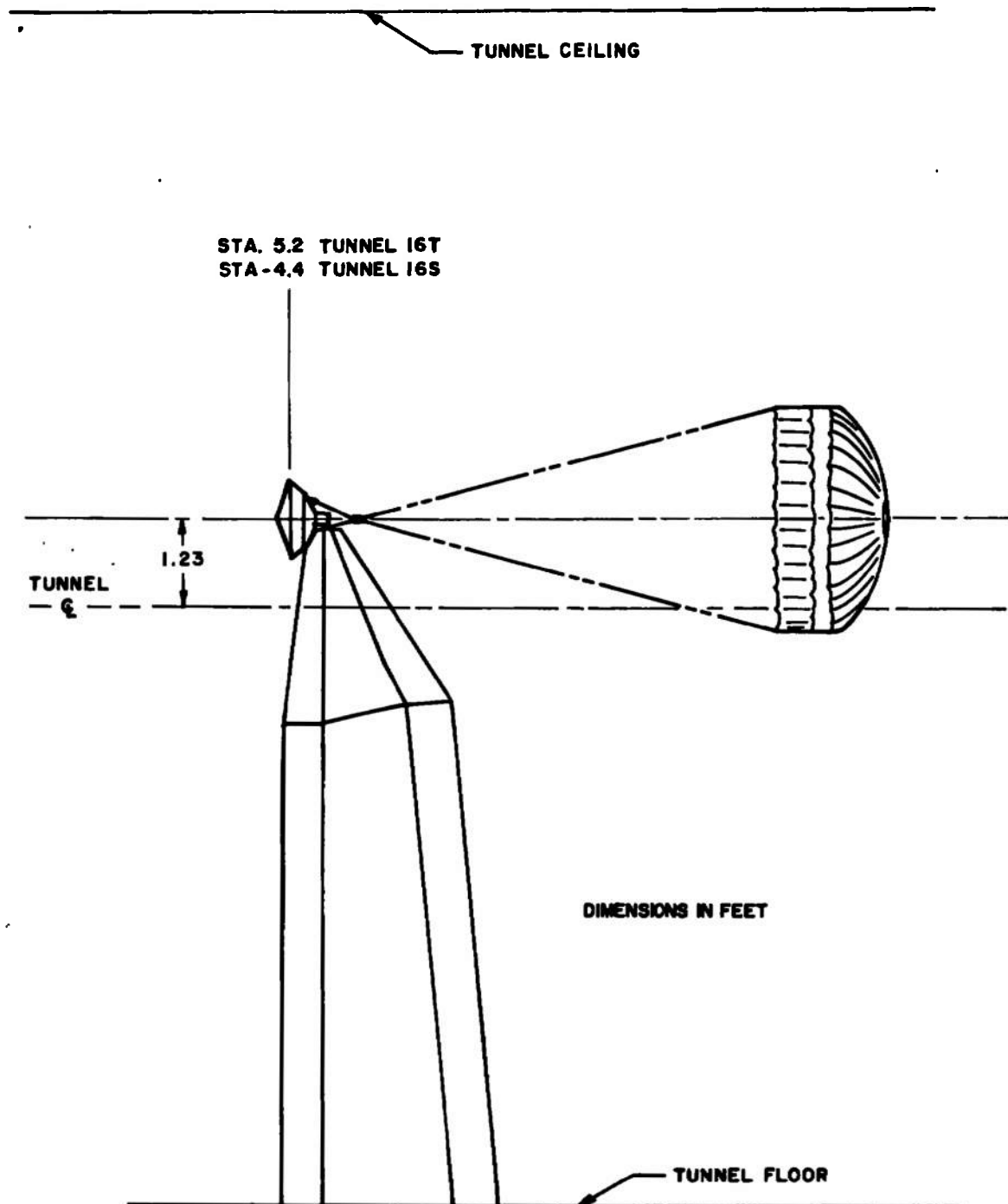
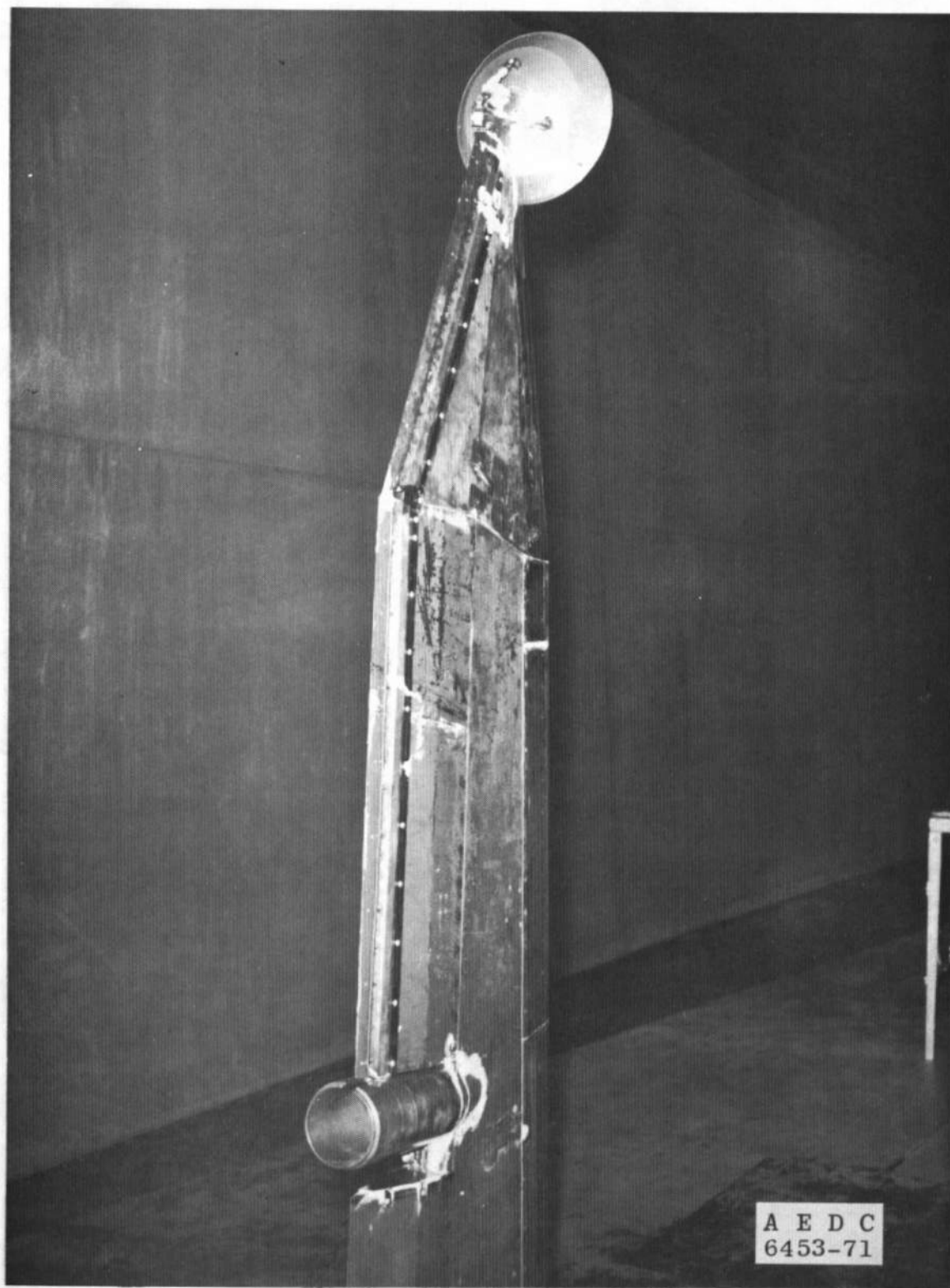


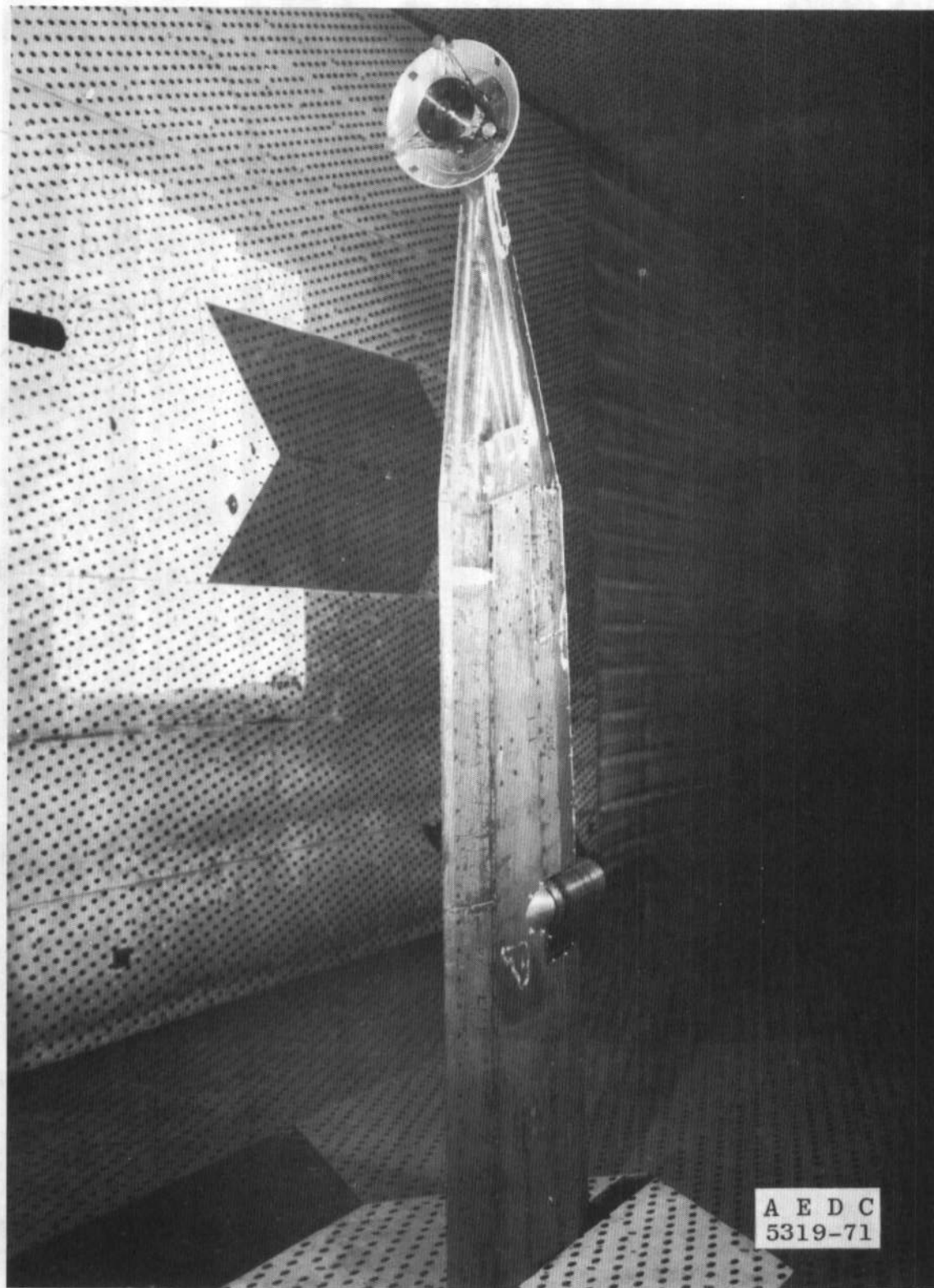
Fig. 1 Sketch of Model Installation



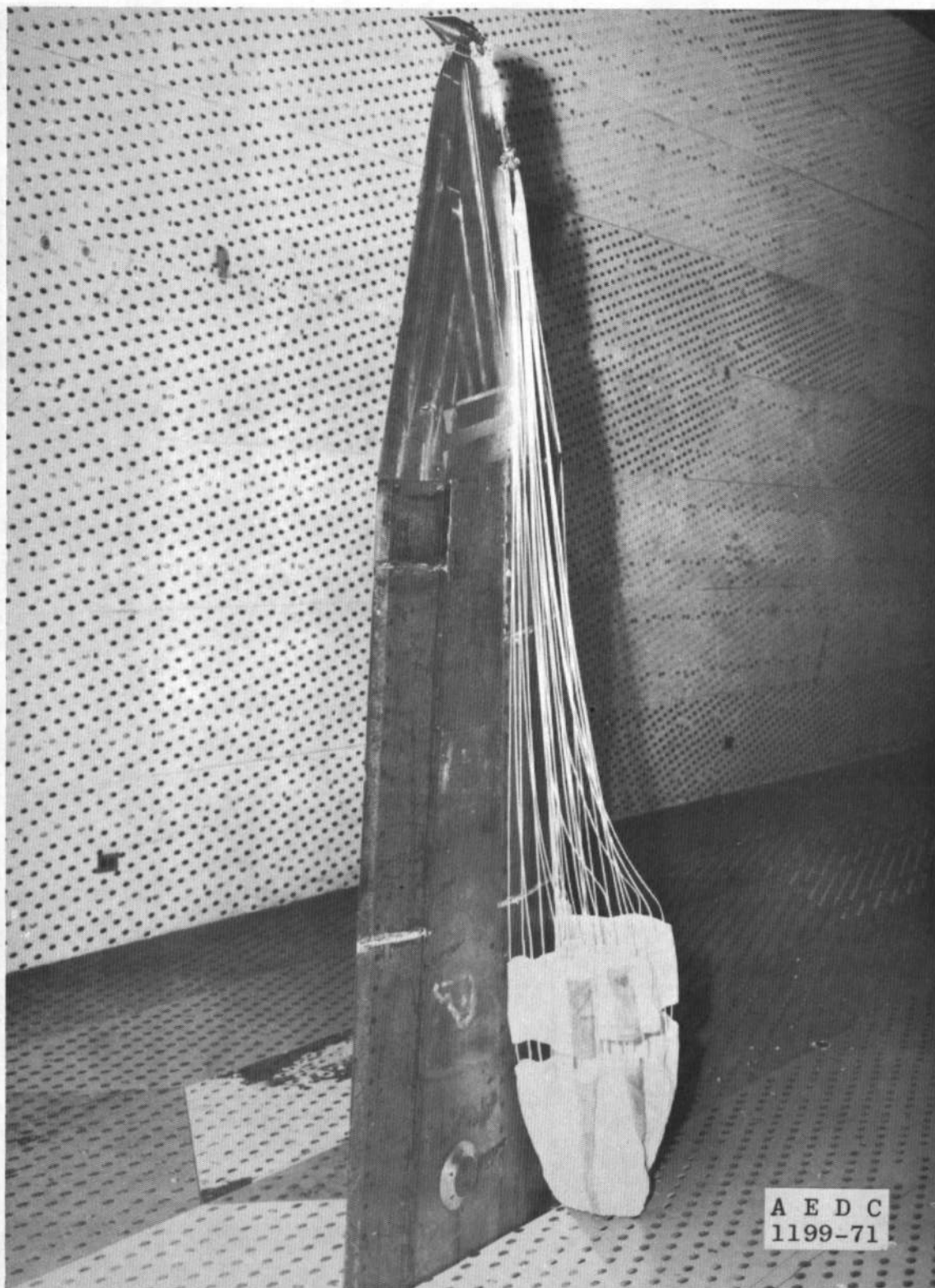
a. Entry Vehicle Model in Tunnel 16S
Fig. 2 Installation Photographs



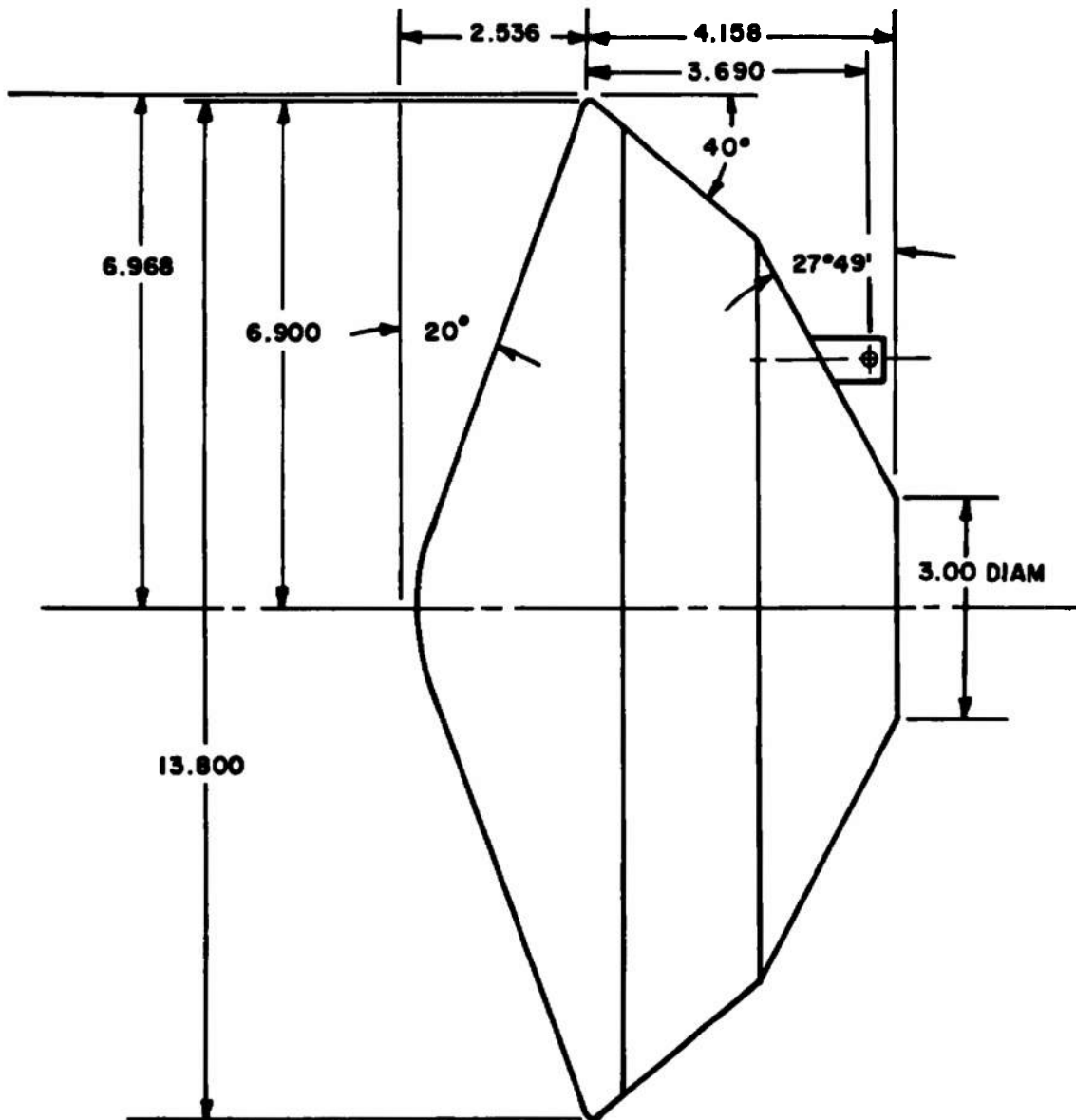
b. Rear Three-Quarter View Showing the Deployment Tube
Fig. 2 Continued



c. Lander Model in Tunnel 16T
Fig. 2 Continued

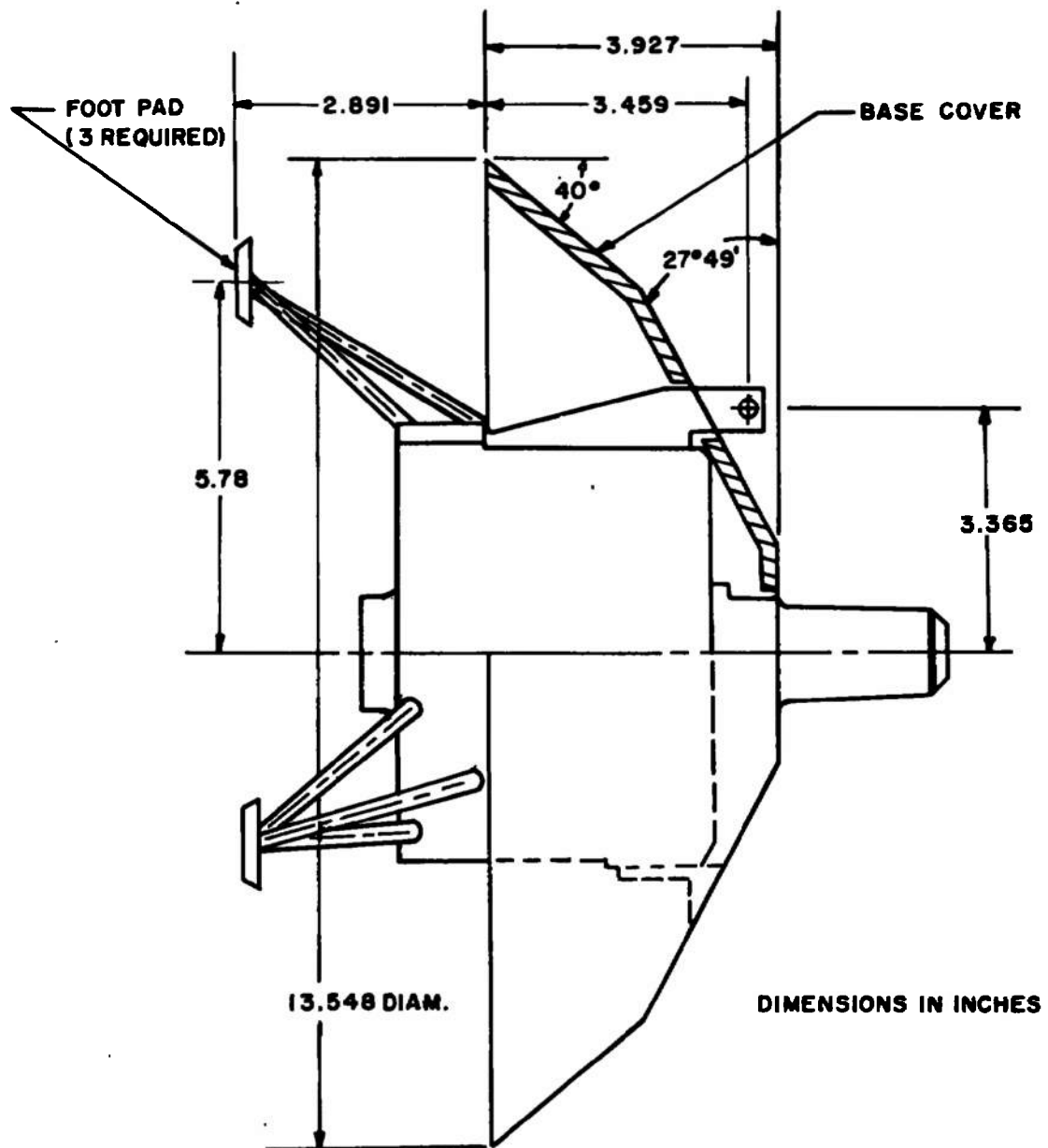


d. Faired Body Model in Tunnel 16T
Fig. 2 Concluded

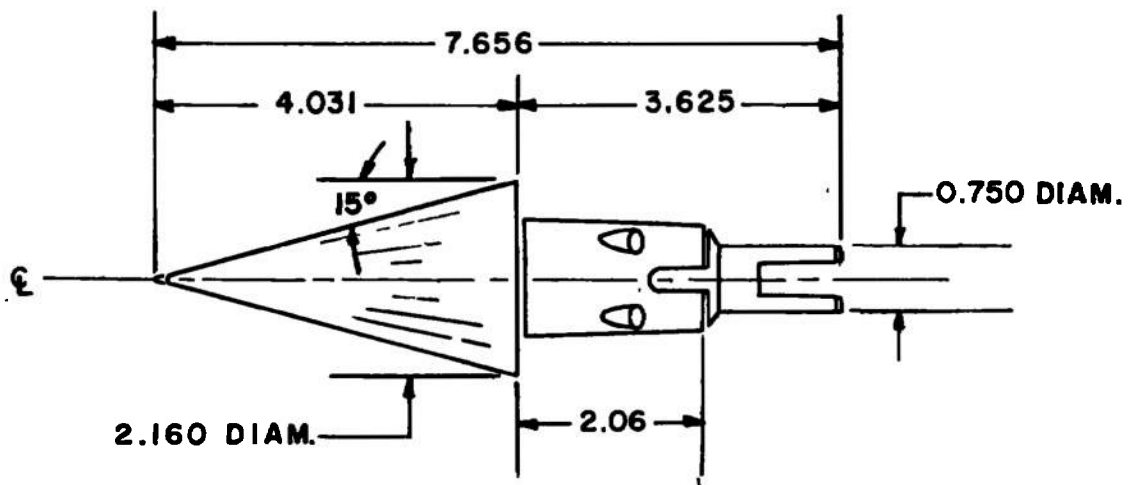


DIMENSIONS IN INCHES

a. Entry Vehicle
Fig. 3 Major Model Details



b. Lander
Fig. 3 Continued



DIMENSIONS IN INCHES

c. Faired Body
Fig. 3 Concluded

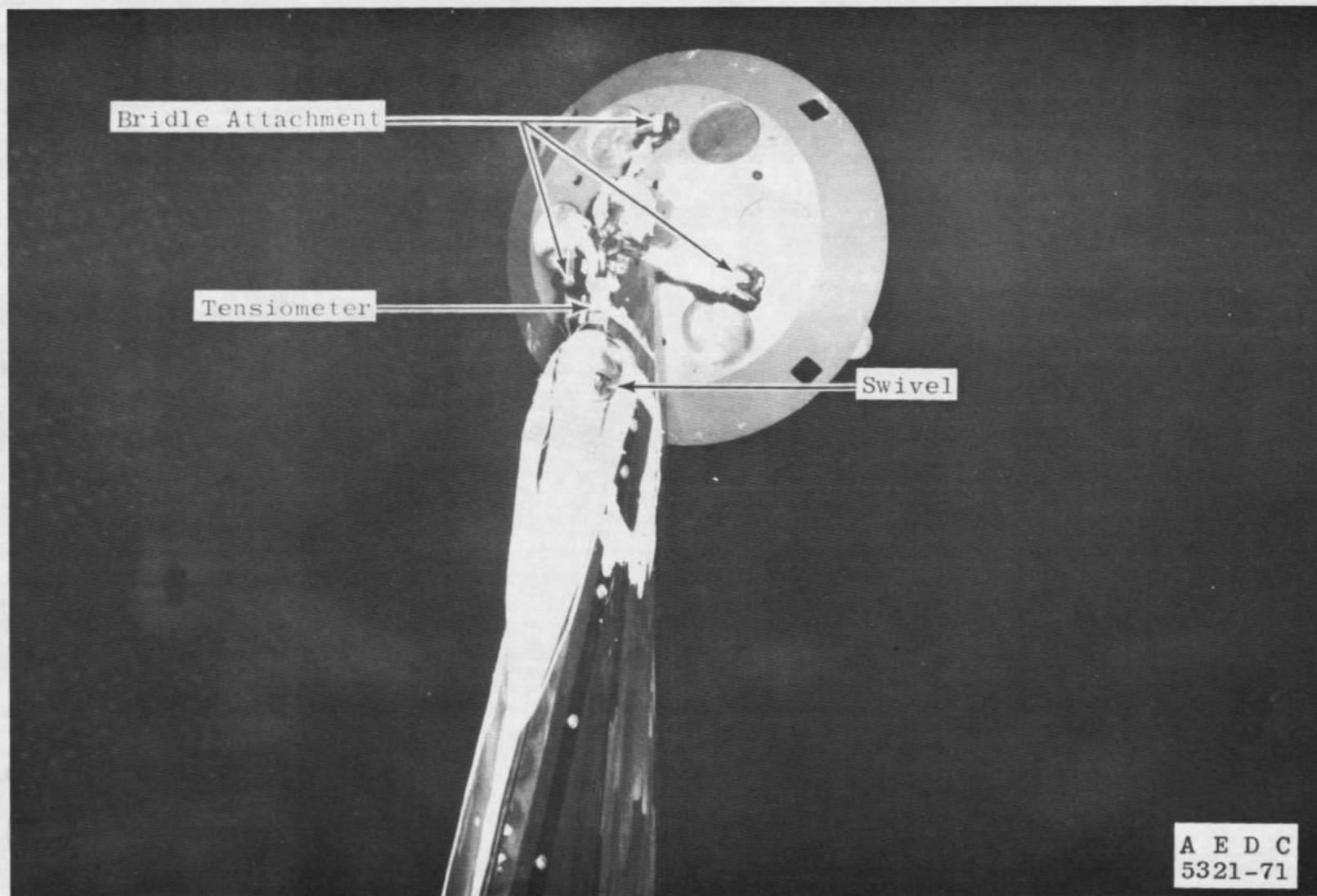
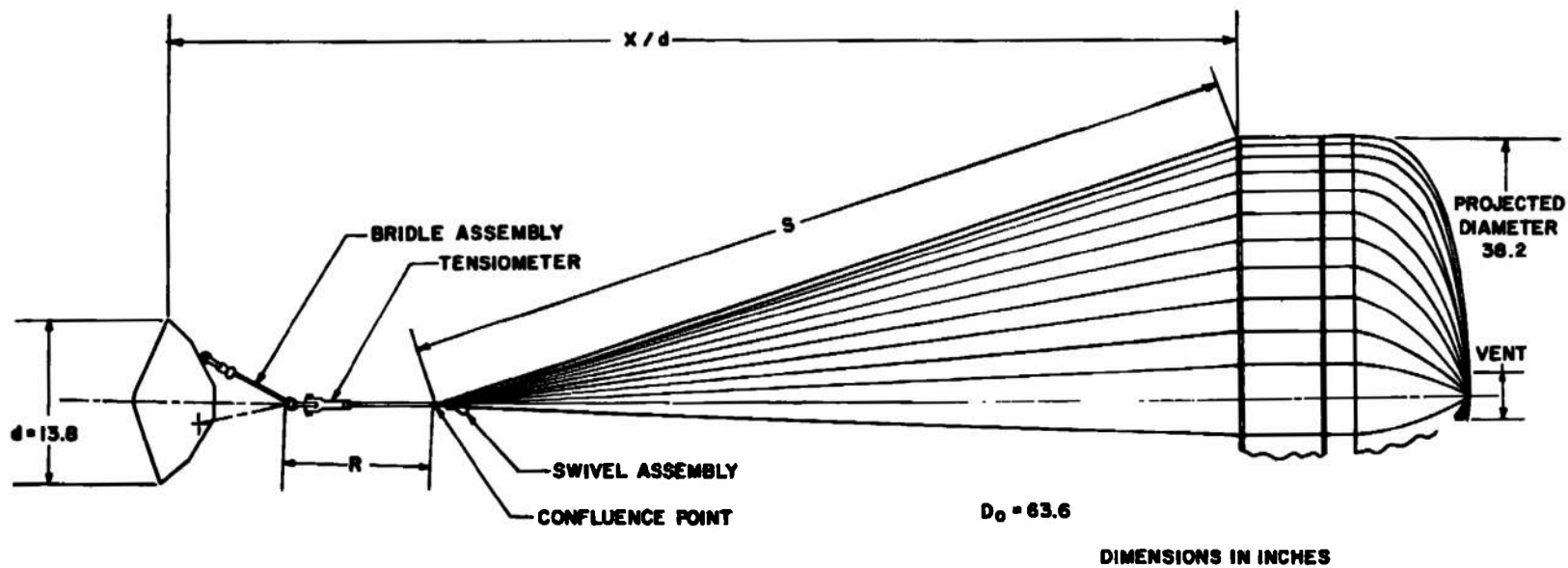


Fig. 4 Photograph of Parachute Attachment



a. Drawing of Parachute Assembly
 Fig. 5 Disk-Gap-Band Parachute Assembly

GEOMETRIC PROPERTIES OF PARACHUTE

<u>Item</u>	<u>Relative Value</u>	<u>Value</u>
Nominal Diameter	D_o	5.3 ft
Total Area (S_o)*	$\pi D_o^2/4$	22.06 ft ²
Geometric Porosity**	0.125 S_o	2.76 ft ²
Disk Area***	0.53 S_o	11.69 ft ²
Disk Diameter	0.726 D_o	3.85 ft
Gap Area	0.12 S_o	2.65 ft ²
Gap Width	0.042 D_o	0.223 ft
Band Area	0.35 S_o	7.72 ft
Band Width	0.121 D_o	0.641 ft
Vent Area	0.005 S_o	0.110 ft ²
Vent Diameter	0.07 D_o	0.371 ft
Number of Suspension Lines	---	48
Thickness of Suspension Lines	0.00011 D_o (FS)	0.07 in.
Thickness of Suspension Lines Actually Tested	0.00157 D_o (model) [†]	0.100 in.
Suspension Line Lengths (S)	1.00 D_o	5.300 ft
	1.16 D_o	6.148 ft
	1.52 D_o	8.056 ft
	1.73 D_o	9.169 ft
	1.85 D_o	9.805 ft
	2.26 D_o	11.980 ft

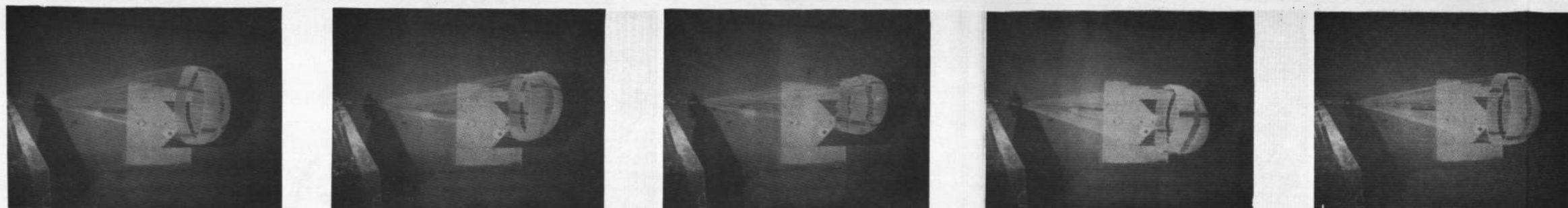
* Disk + Gap + Band

** Gap + Vent provide 12.5 percent geometric porosity

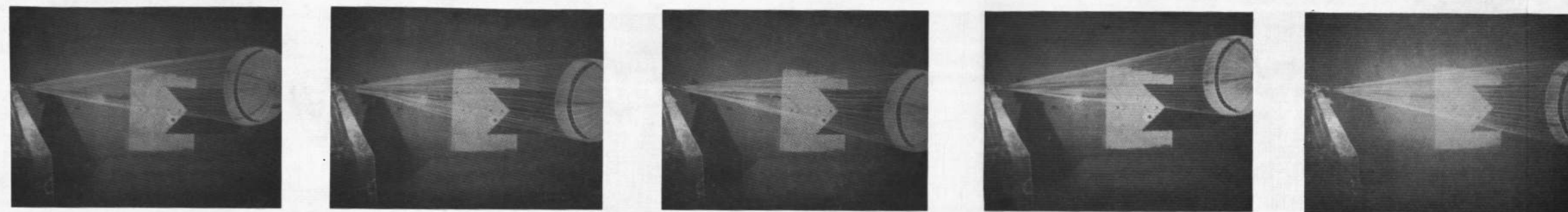
*** Includes Vent

† Based on wide edge dimension

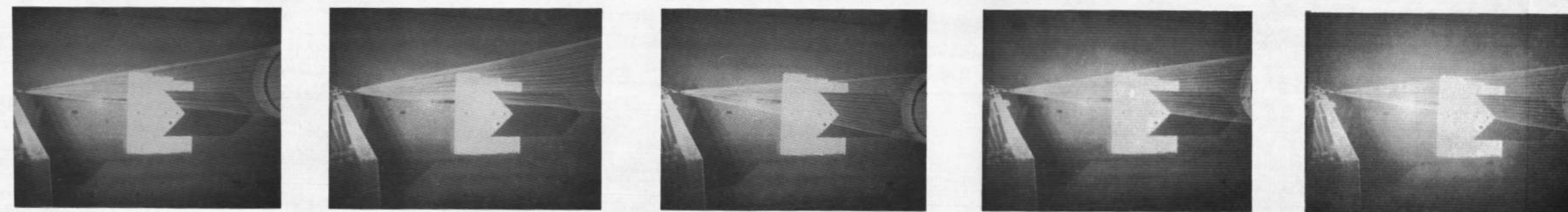
b. Geometric Properties of Parachute
Fig. 5 Concluded



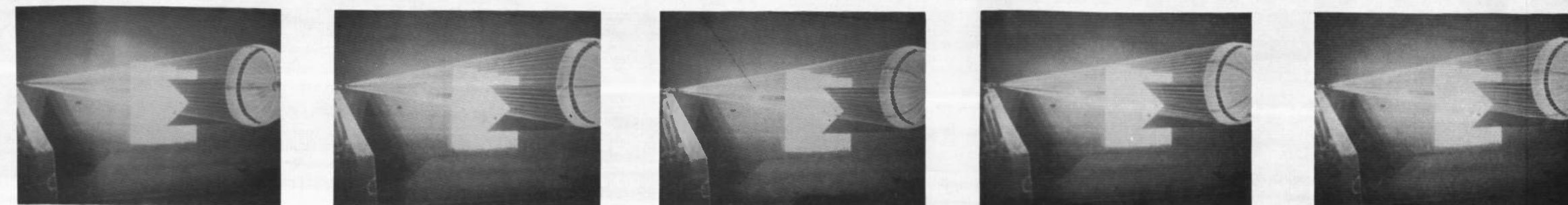
Configuration 2
X/d = 6.50
Lander Forebody



Configuration 5
X/d = 9.14
Lander Forebody



Configuration 6
X/d = 11.02
Entry Vehicle Forebody



Configuration 5
X/d = 9.14
Faired Forebody

$M_\infty = 0.6$

$M_\infty = 0.8$

$M_\infty = 1.0$

$M_\infty = 1.2$

$M_\infty = 1.4$

Fig. 6 Photographs of the Disk-Gap-Band Parachute at Various Trailing Distances and Mach Numbers

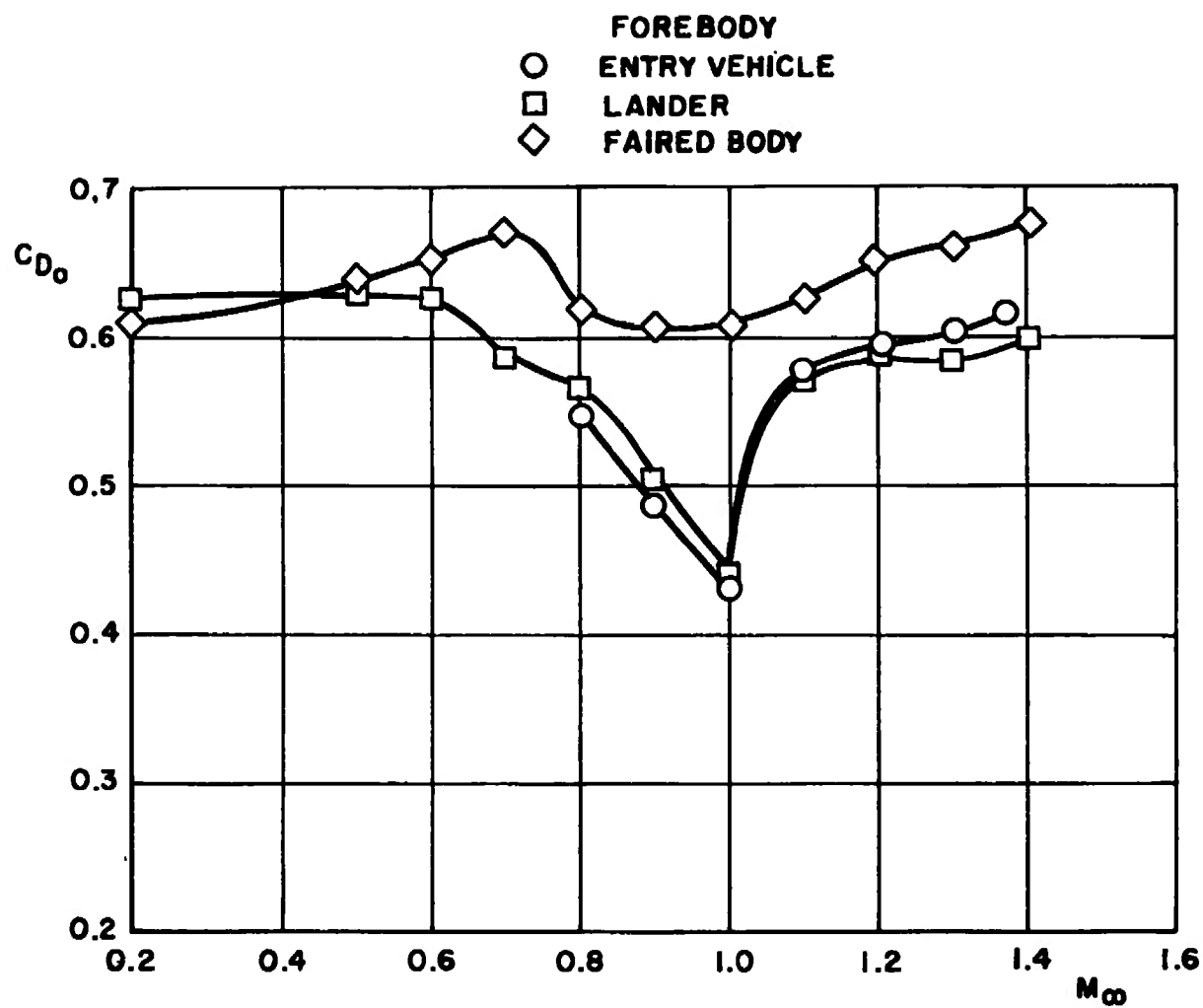
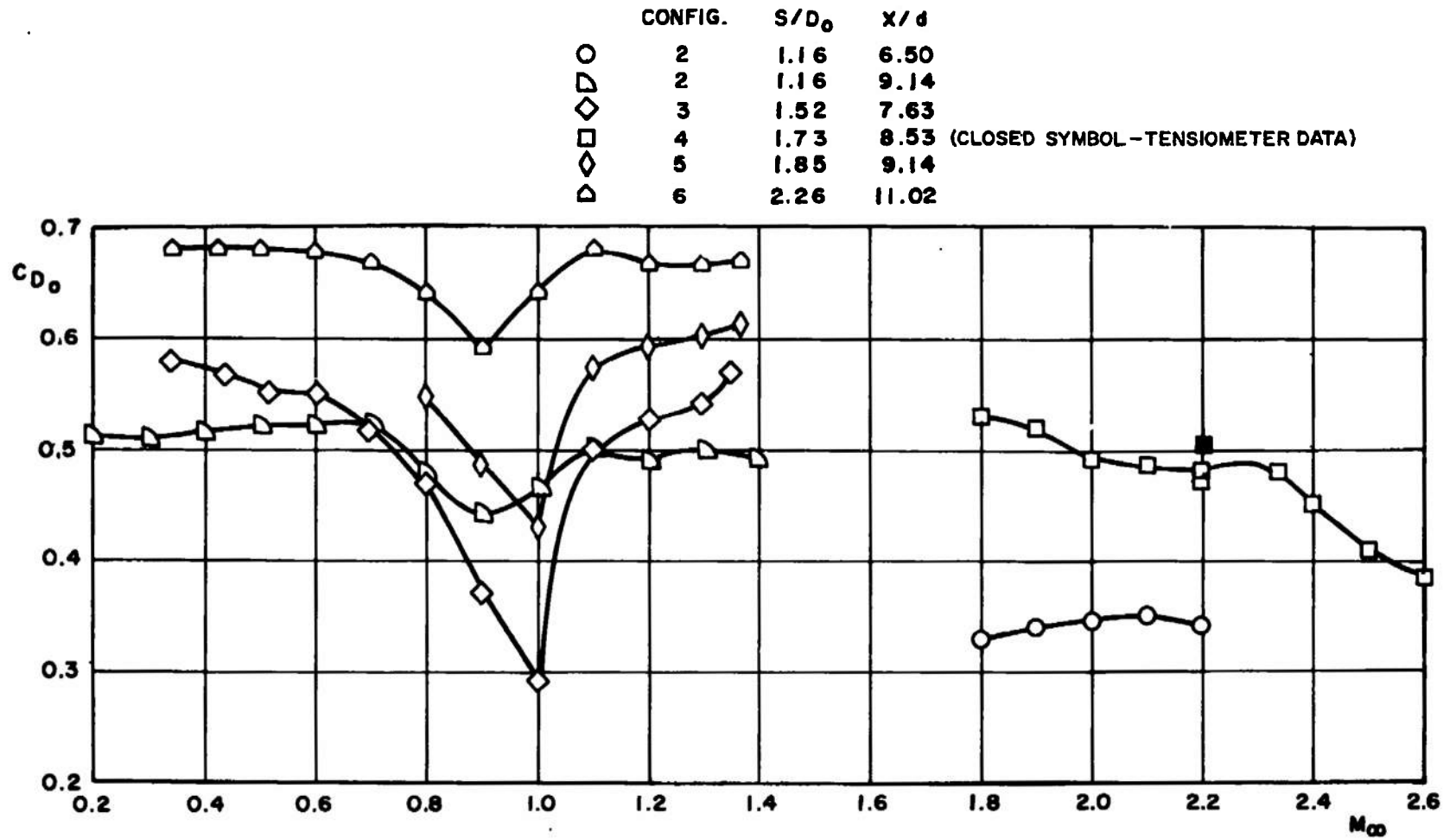


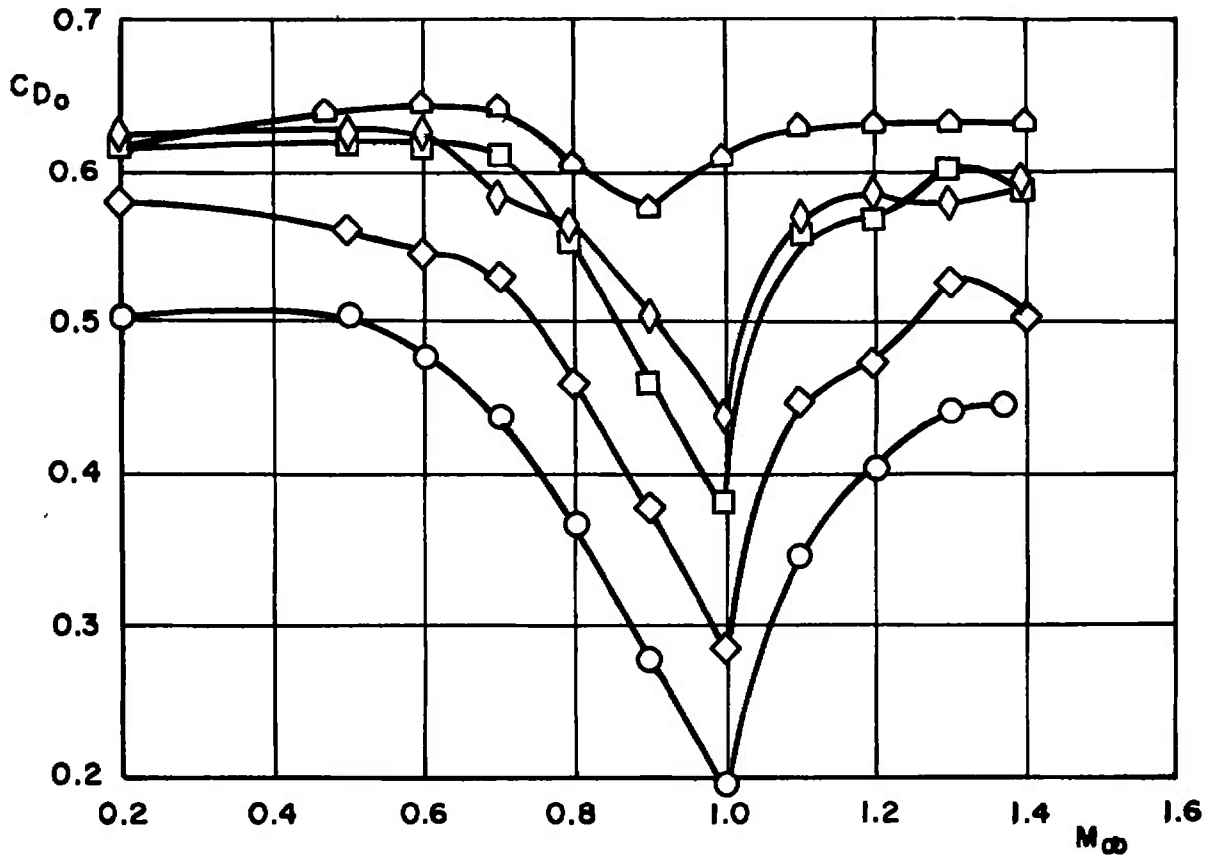
**Fig. 7 Effect of Forebody Shape on the Parachute Drag Coefficient,
 $S/D_0 = 1.85$, $X/d = 9.14$**



a. Entry Vehicle Forebody

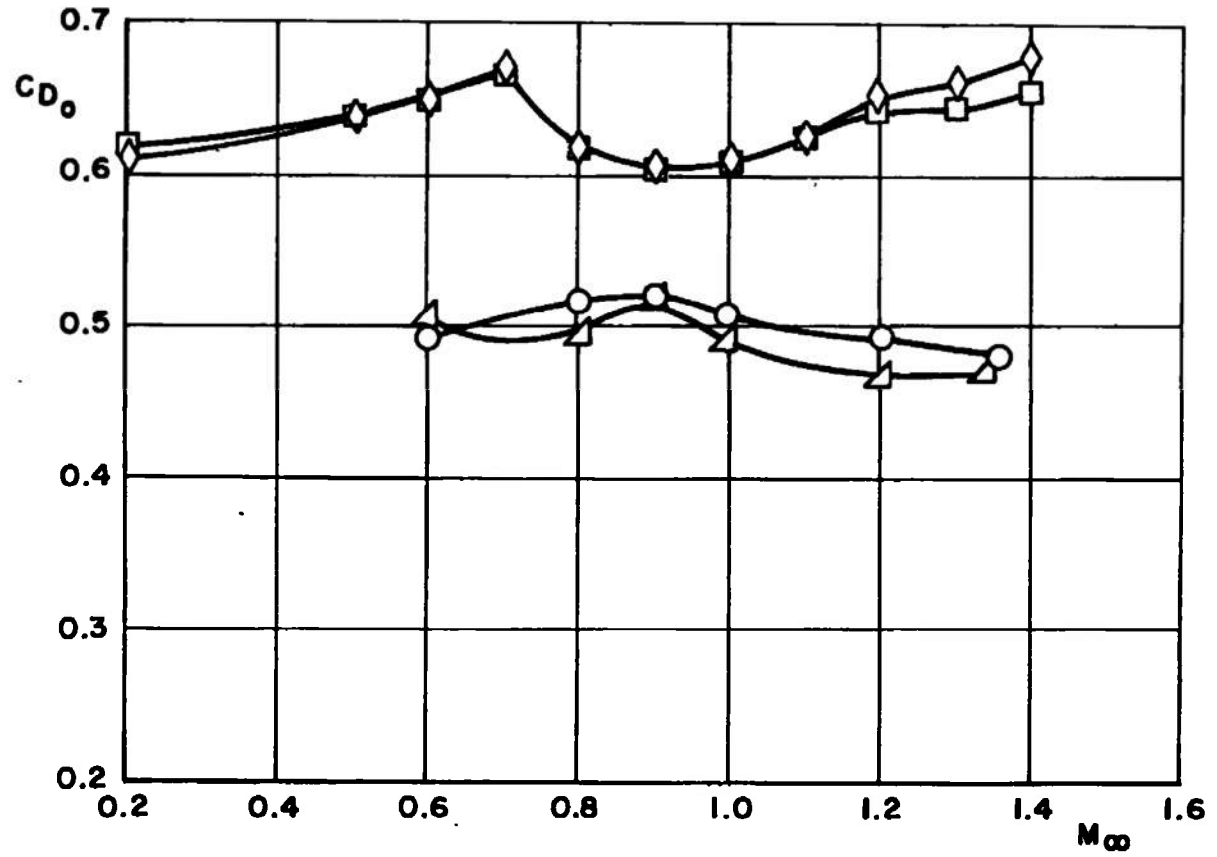
Fig. 8 Variation of Parachute Drag Coefficient with Free-Stream Mach Number

	CONFIG.	S/D ₀	X/d
○	2	1.16	6.50
◇	3	1.52	7.63
□	4	1.73	8.53
◇	5	1.85	9.14
△	6	2.26	11.02



b. Lander Forebody
Fig. 8 Continued

	CONFIG.	S/D _o	X/d
△	1	1.00	4.70
○	2	1.16	4.70
□	4	1.73	8.53
◇	5	1.85	9.14



c. Faired Forebody
Fig. 8 Concluded

TABLE I
SUMMARY OF PARACHUTE TEST CONDITIONS AND PERFORMANCE RESULTS

Parachute Configuration	Forebody Configuration	M_∞	q_∞ , psf	S/D_0	X/d	C_{D_0}	Observations
1	Faired Body	0.60	100.4	1.00		0.507	Very stable and well inflated, little or no canopy pulsing
		0.80	100.2			0.492	Same as $M_\infty = 0.6$
		0.90	100.2			0.514	Same as $M_\infty = 0.6$
		1.00	101.5			0.490	Same as $M_\infty = 0.6$
		1.20	100.2			0.467	Same as $M_\infty = 0.6$
		1.37	100.5			0.471	Same as $M_\infty = 0.6$
2	Faired Body	0.60	100.0	1.16		0.490	Very stable and well inflated; little or no canopy pulsing
		0.80	99.5			0.512	Same as $M_\infty = 0.6$
		0.90	101.0			0.517	Same as $M_\infty = 0.6$
		1.00	100.8			0.504	Same as $M_\infty = 0.6$
		1.20	99.0			0.493	Same as $M_\infty = 0.6$
		1.38	100.1			0.487	Same as $M_\infty = 0.6$
2	Lander	1.37	80.0	1.16	6.50	0.446	Stable and well inflated, light canopy pulsing
		1.30	80.0			0.440	Same as $M_\infty = 1.38$ except medium canopy pulsing
		1.20	80.2			0.405	Fair stability and fair inflation, intermittent squidding
		1.10	80.0			0.345	Fair stability and poor inflation, intermittent heavy squidding
		1.00	80.3			0.193	Stable and very poor inflation, canopy assumed a full reefed condition
		0.90	79.7			0.275	Stable and poor inflation, intermittent heavy squidding
		0.80	79.1			0.365	Fair stability and fair inflation, light squidding
		0.70	80.2			0.437	Stable and well inflated
		0.60	78.6			0.474	Same as $M_\infty = 0.70$
		0.50	79.4			0.504	Very stable and well inflated, light pulsing
		0.20	56.7			0.505	Same as $M_\infty = 0.50$
2	Entry Vehicle	2.20	77.8	1.16	6.50	0.341	Fair stability and poor inflation, intermittent heavy squidding
		2.10	78.9			0.350	Same as $M_\infty = 2.20$
		2.00	79.3			0.347	Fair stability and fair inflation, intermittent canopy pulsing
		1.90	81.0			0.339	Fair stability and well inflated, medium canopy pulsing
		1.80	80.2			0.330	Same as $M_\infty = 1.90$

TABLE I. (Continued)

Parachute Configuration	Forebody Configuration	M_∞	q_∞ , psf	S/D_0	X/d	C_{D_0}	Observations
2	Entry Vehicle	1.40	80.0	1.16	9.14	0.490	Stable and well inflated, light canopy pulsing
		1.30	80.2			0.498	Same as $M_\infty = 1.40$
		1.20	80.4			0.489	Fair stability and fair inflation, intermittent squidding
		1.10	80.2			0.500	Stable and well inflated
		1.00	79.6			0.466	Fair stability and well inflated
		0.90	80.3			0.440	Stable and well inflated
		0.80	79.2			0.481	Same as $M_\infty = 0.90$
		0.70	80.3			0.520	Same as $M_\infty = 0.90$
		0.60	79.9			0.521	Very stable and well inflated
		0.50	75.8			0.521	Same as $M_\infty = 0.60$
		0.20	67.0			0.514	Same as $M_\infty = 0.60$
3	Entry Vehicle	1.35	85.3	1.52	7.63	0.571	Very stable and well inflated
		1.30	83.0			0.542	Stable and well inflated, light canopy pulsing
		1.20	80.4			0.527	Same as $M_\infty = 1.30$
		1.10	80.3			0.501	Fair stability and fair inflation, intermittent squidding
		1.00	80.8			0.293	Fair stability and poor inflation, heavy squidding
		0.90	80.3			0.370	Same as $M_\infty = 1.00$
		0.80	80.0			0.470	Stable and well inflated
		0.70	79.4			0.515	Same as $M_\infty = 0.80$
		0.60	80.0			0.550	Same as $M_\infty = 0.80$
		0.52	73.3			0.551	Same as $M_\infty = 0.80$
3	Lander	1.40	79.8	1.52	7.63	0.504	Very stable and well inflated
		1.30	80.4			0.527	Same as $M_\infty = 1.40$ with slight canopy pulsing
		1.20	82.0			0.474	Fair stability and well inflated, heavy canopy pulsing
		1.10	79.6			0.447	Same as $M_\infty = 1.20$ with intermittent squidding
		1.00	80.0			0.284	Fair stability and poor inflation, continuous squidding
		0.90	80.1			0.377	Fair stability and fair inflation, intermittent squidding

TABLE I (Continued)

Parachute Configuration	Forebody Configuration	M_∞	q_∞ , psf	S/D_0	X/d	C_{D_0}	Observations
3	Lander	0.80	79.8	1.52	7.63	0.458	Stable and well inflated, medium canopy pulsing
		0.70	79.8			0.531	Good Stability and well inflated
		0.60	80.6			0.544	Same as $M_\infty = 0.70$
		0.50	79.2			0.562	Same as $M_\infty = 0.70$
		0.20	56.1			0.582	Same as $M_\infty = 0.70$
4	Lander	1.40	81.1	1.73	8.53	0.590	Very stable and well inflated
		1.30	80.7			0.602	Same as $M_\infty = 1.40$
		1.20	80.7			0.569	Stable and well inflated
		1.10	81.2			0.556	Stable and fair inflation, intermittent squidding
		1.00	81.4			0.379	Stable and poor inflation, heavy squidding
		0.90	80.2			0.460	Fair stability and fair inflation, intermittent squidding
		0.80	80.0			0.552	Fair stability and well inflated, slow parachute oscillations
		0.70	79.8			0.610	Same as $M_\infty = 0.80$
		0.60	79.7			0.613	Same as $M_\infty = 0.80$
		0.50	80.2			0.619	Same as $M_\infty = 0.80$
		0.20	60.0			0.618	Same as $M_\infty = 0.80$
4	Entry Vehicle	2.60	70.5	1.73	8.53	0.379	Fair stability inflation, medium squidding
		2.40	70.0			0.449	Poor stability and poor inflation, heavy squidding
		2.20	79.8			0.480	Fair stability and fair inflation, intermittent squidding
		2.10	78.6			0.486	Same as $M_\infty = 2.20$
		2.00	78.5			0.491	Same as $M_\infty = 2.20$
		1.90	78.6			0.519	Stable and well inflated
		1.80	79.0			0.528	Same as $M_\infty = 1.90$
4	Faired Body	0.22	59.7	1.73	8.53	0.618	Stable and well inflated
		0.50	79.0			0.637	Same as $M_\infty = 0.20$
		0.60	79.0			0.651	Same as $M_\infty = 0.20$
		0.70	80.0			0.667	Same as $M_\infty = 0.20$
		0.80	79.8			0.616	Same as $M_\infty = 0.20$
		0.90	80.1			0.602	Same as $M_\infty = 0.20$
		1.00	80.0			0.809	Same as $M_\infty = 0.20$
		1.10	80.0			0.624	Same as $M_\infty = 0.20$

TABLE I (Continued)

Parachute Configuration	Forebody Configuration	M_∞	q_∞ , psf	S/D_0	X/d	C_{D_0}	Observations
4	Faired Body	1.20	80.7	1.73	8.53	0.641	Same as $M_\infty = 0.20$
4	Faired Body	1.30	79.2	1.73	8.53	0.643	Very stable and well inflated, light pulsing
4	Faired Body	1.40	80.3	1.73	8.53	0.657	Very stable and well inflated
5	Entry Vehicle	1.37	85.3	1.85	9.14	0.615	Very stable and well inflated
↓	↓	1.30	80.2	↓	↓	0.600	Same as $M_\infty = 1.40$
↓	↓	1.20	80.2	↓	↓	0.593	Stable and well inflated
↓	↓	1.10	79.2	↓	↓	0.576	Same as $M_\infty = 1.20$
↓	↓	1.00	79.1	↓	↓	0.425	Stable and fair inflation, heavy canopy pulsing
↓	↓	0.90	79.5	↓	↓	0.486	Same as $M_\infty = 1.0$
↓	↓	0.80	78.6	↓	↓	0.546	Stable and well inflated, medium canopy pulsing (swivel connection failed)
5	Lander	1.40	80.5	1.85	9.14	0.590	Very stable and well inflated
↓	↓	1.30	80.5	↓	↓	0.580	Same as $M_\infty = 1.40$
↓	↓	1.20	79.7	↓	↓	0.585	Stable and well inflated, light canopy pulsing
↓	↓	1.10	79.5	↓	↓	0.568	Fair stability and well inflated, medium canopy pulsing
↓	↓	1.00	79.6	↓	↓	0.438	Fair stability and fair inflation, intermittent squidding
↓	↓	0.90	80.0	↓	↓	0.503	Same as $M_\infty = 1.00$
↓	↓	0.80	79.9	↓	↓	0.564	Stable and well inflated, medium canopy pulsing
↓	↓	0.70	80.3	↓	↓	0.583	Stable and well inflated
↓	↓	0.60	79.6	↓	↓	0.625	Same as $M_\infty = 0.70$
↓	↓	0.50	80.0	↓	↓	0.625	Same as $M_\infty = 0.70$
↓	↓	0.20	54.5	↓	↓	0.625	Same as $M_\infty = 0.70$
5	Faired Body	0.20	58.3	1.85	8.53	0.614	Stable and well inflated, slow intermittent oscillations
↓	↓	0.50	80.1	↓	↓	0.638	Same as $M_\infty = 0.2$
↓	↓	0.60	80.2	↓	↓	0.651	
↓	↓	0.70	79.5	↓	↓	0.670	
↓	↓	0.80	80.4	↓	↓	0.616	
↓	↓	0.90	79.4	↓	↓	0.606	
↓	↓	1.00	79.5	↓	↓	0.609	
↓	↓	1.10	80.4	↓	↓	0.626	
↓	↓	1.20	79.5	↓	↓	0.652	Very stable and well inflated
↓	↓	1.30	80.3	↓	↓	0.663	Excellent stability and inflation
↓	↓	1.40	80.0	↓	↓	0.678	Same as $M_\infty = 1.30$

TABLE I (Concluded)

Parachute Configuration	Forebody Configuration	M_∞	q_∞ , psf	S/D_0	X/d	C_{D_0}	Observations
6	Entry Vehicle	1.37	79.5	2.26	11.02	0.668	Excellent stability and inflation
		1.30	79.9			0.664	Same as $M_\infty = 1.40$
		1.20	80.1			0.665	Very stable and well inflated
		1.10	79.6			0.678	Stable and well inflated
		1.00	80.4			0.640	Same as $M_\infty = 1.10$ with light canopy pulsing
		0.90	79.7			0.592	Same as $M_\infty = 1.00$
		0.80	80.5			0.639	Same as $M_\infty = 1.00$
		0.70	80.1			0.667	Stable and well inflated
		0.60	80.0			0.678	Same as $M_\infty = 0.70$
		0.50	80.0			0.681	Same as $M_\infty = 0.70$
	Lander	1.40	78.8	2.26	11.02	0.631	Very stable and well inflated
		1.30	80.3			0.632	Same as $M_\infty = 1.40$
		1.20	80.4			0.630	Stable and well inflated, light canopy pulsing
		1.10	80.1			0.630	Same as $M_\infty = 1.20$
		1.00	80.2			0.608	
		0.90	80.2			0.576	
		0.80	80.1			0.602	
		0.70	80.3			0.644	
		0.60	79.6			0.643	
		0.50	79.5			0.637	
		0.20	59.5			0.618	

UNCLASSIFIED

Security Classification

DOCUMENT CONTROL DATA - R & D

(Security classification of title, body of abstract and indexing annotation must be entered when the overall report is classified)

1. ORIGINATING ACTIVITY (Corporate author)

Arnold Engineering Development Center
Arnold Air Force Station, Tennessee 37389

2a. REPORT SECURITY CLASSIFICATION

UNCLASSIFIED

2b. GROUP

N/A

3. REPORT TITLE

AERODYNAMIC CHARACTERISTICS OF DISK-GAP-BAND PARACHUTES IN THE
WAKE OF VIKING ENTRY FOREBODIES AT MACH NUMBERS FROM 0.2 TO 2.6

4. DESCRIPTIVE NOTES (Type of report and inclusive dates)

Final Report - June 29 to August 13, 1971

5. AUTHOR(S) (First name, middle initial, last name)

David E. A. Reichenau, ARO, Inc.

6. REPORT DATE

July 1972

7a. TOTAL NO. OF PAGES

37

7b. NO. OF REFS

1

8a. CONTRACT OR GRANT NO.

b. PROJECT NO.

c. Program Element 921E

d.

9a. ORIGINATOR'S REPORT NUMBER(S)

AEDC-TR-72-78

9b. OTHER REPORT NO(S) (Any other numbers that may be assigned this report)

ARO-PWT-TR-71-192

10. DISTRIBUTION STATEMENT

Approved for public release; distribution unlimited.

11. SUPPLEMENTARY NOTES

Available in DDC

12. SPONSORING MILITARY ACTIVITY

NASA Langley Research Center
Viking Project Office, Mail Stop 159
Hampton, Virginia 23365

13. ABSTRACT

Tests were conducted in the Propulsion Wind Tunnels (16T) and (16S) to determine the drag and performance characteristics of various disk-gap-band parachute configurations in the wake of a 0.10-scale Viking entry vehicle. The parachutes were also tested behind a small faired body to obtain minimum interference parachute performance characteristics. The results show that in general the parachutes had good inflation and stability characteristics in the wake of the entry forebodies at Mach numbers from 0.2 to 0.8 and from 1.2 to 2.0. Considerable loss in parachute performance was experienced in the wake of the forebodies in the vicinity of Mach number 1.0. Increasing the parachute trailing distance and suspension line length increased the parachute drag coefficient at each Mach number.

14.	KEY WORDS	LINK A		LINK B		LINK C	
		ROLE	WT	ROLE	WT	ROLE	WT
	parachutes - - <i>Performance</i>						
	entry vehicles						
	VIKING spacecraft						
	Mars (planet)						
	drag						
	performance characteristics						
	stability						
	wind tunnels						
	transonic flow						
	supersonic flow						
	subsonic flow						
	2. Parachutes - - <i>Drag</i>						
	3. Disk - gap - band <i>parachutes</i>						